



HAL
open science

Aliasing in Micro Rain Radar data due to strong vertical winds

F. Tridon, Joël van Baelen, Y. Pointin

► **To cite this version:**

F. Tridon, Joël van Baelen, Y. Pointin. Aliasing in Micro Rain Radar data due to strong vertical winds. Geophysical Research Letters, 2011, 38 (2), pp.n/a-n/a. 10.1029/2010GL046018 . hal-02092533

HAL Id: hal-02092533

<https://uca.hal.science/hal-02092533>

Submitted on 24 Aug 2021

HAL is a multi-disciplinary open access archive for the deposit and dissemination of scientific research documents, whether they are published or not. The documents may come from teaching and research institutions in France or abroad, or from public or private research centers.

L'archive ouverte pluridisciplinaire **HAL**, est destinée au dépôt et à la diffusion de documents scientifiques de niveau recherche, publiés ou non, émanant des établissements d'enseignement et de recherche français ou étrangers, des laboratoires publics ou privés.

Copyright

Aliasing in Micro Rain Radar data due to strong vertical winds

F. Tridon,^{1,2} J. Van Baelen,^{1,2} and Y. Pointin^{1,2}

Received 29 October 2010; revised 25 November 2010; accepted 3 December 2010; published 25 January 2011.

[1] Vertically pointing Micro Rain Radars (MRRs) provide profiles of drop size distributions (DSDs) from the measured Doppler reflectivity spectra. However, in the presence of strong vertical winds, the measured spectra can suffer from aliasing errors. These errors can considerably affect the derived DSD, and hence, the retrieved rain parameters. In this work, we show that such aliasing can be automatically detected and that this detection can be used at our benefit to identify strong vertical winds and eliminate incorrect retrievals. Likewise, we show that when this aliasing is adequately corrected, the retrieved DSD is then fit for further parameter retrievals. **Citation:** Tridon, F., J. Van Baelen, and Y. Pointin (2011), Aliasing in Micro Rain Radar data due to strong vertical winds, *Geophys. Res. Lett.*, 38, L02804, doi:10.1029/2010GL046018.

1. Introduction

[2] The measurement of drop size distribution (DSD) from vertically pointing radars has been investigated since the early days of radar meteorology. The Doppler spectra obtained reflect the fall velocity distribution of hydrometeors and can be converted into DSDs under the assumption of no vertical wind. Not only, this is the only way to determine vertical profiles of DSDs but also, it allows for more representative measurements given its rather large sampling volume compared to the conventional measurements with disdrometers or in-situ probes. With the advent of Micro Rain Radars (MRRs) [Peters *et al.*, 2005], this technique is the object of renewed interest. However, it is known that it suffers limitations due to vertical wind and turbulence.

[3] Several methods have been proposed to estimate simultaneously from a single vertically pointing Doppler radar, the wind intensity and the DSD [Battan, 1964; Rogers, 1967; Hauser and Amayenc, 1981], and the turbulence [Wakasugi *et al.*, 1987; Gossard, 1994; Babb *et al.*, 2000].

[4] As shown by Peters *et al.* [2005], the turbulence can broaden the spectra measured by MRRs and have a non-negligible impact on the retrieved parameters. However, the proposed corrections are based on simplification hypothesis and have not been applied here because it is out of the scope of this study and this won't affect the overall results.

[5] Furthermore, as indicated by Atlas *et al.* [1973], the techniques for vertical wind correction present some constraints, as they require assumptions on the size of the smallest detectable hydrometeors or on the shape of the DSD. In addition, errors in the vertical wind estimation will induce

shifts of the reflectivity spectrum with respect to the drop diameter D and given the large reflectivity sensitivity to DSD (i.e., proportional to D^6), a reasonable error on the estimation of the vertical wind will then lead to unacceptable errors in the number concentration. Then, a vertical wind correction might even deteriorate the quality of rain parameters estimates. That is the reason why the assumption of no vertical wind is usually made for the MRR measurements. Furthermore, from both the theoretical and experimental points of view, Peters *et al.* [2005] showed that, as long as the vertical wind is not too large (lower than 2 m s^{-1}), the MRR data averaged over 1 min intervals provide good estimates of the actual DSD and rain parameters without vertical wind correction.

[6] However, in case of stronger vertical winds, the instantaneous MRR retrievals can be dramatically affected due to aliasing of the spectra.

[7] In this work, after a quick presentation of the operational mode of the MRR, we study the impact of such strong vertical winds on the measured reflectivity spectra. We show that such aliasing indicates strong updraft or downdraft and can act as a warning to detect incorrect DSDs. Then, we investigate its impact on the derived DSD and on the retrieved parameters. Finally, we summarize our results and discuss how the aliasing detection can contribute to reliable MRR retrievals.

2. Operation Mode of the MRRs

[8] The MRR is a vertically looking FM-CW K-band radar (24 GHz) which derives Doppler spectra of 63 bins from 0 to 12 m s^{-1} over 32 range gates with 100 m vertical resolution every 10 seconds. The spectral reflectivity is dynamically analyzed to estimate and remove noise. Afterwards, the relationship of Atlas *et al.* [1973] is used to convert the terminal fall velocity v (m s^{-1}) corrected from air density effect, in diameter D (mm) within the range limits of $D_{\min} = 0.246 \text{ mm}$ and $D_{\max} = 5.8 \text{ mm}$ corresponding to $v_{\min} = 0.76 \text{ m s}^{-1}$ and $v_{\max} = 9.36 \text{ m s}^{-1}$, respectively. Then, assuming that drops are oblate spheroids of equivalent diameter D , the single particle backscattering cross section is calculated under Mie theory and used to derive the corresponding profiles of DSDs. Finally, these DSDs provide the profiles of radar reflectivity factor Z ($\text{mm}^6 \text{ m}^{-3}$), rain rate R (mm h^{-1}) and attenuation coefficient k (dB km^{-1}). In addition, k is used to correct for the attenuation along the path by using the finite-range resolution method of Peters *et al.* [2010] as an improvement over the Hitschfeld and Bordan [1954] algorithm. This method is restricted to attenuation coefficient below 21 dB km^{-1} .

3. Aliasing on MRR Spectra

[9] In this section, we use a small convective shower on 16 June 2007 between 11:30 and 11:45 UTC as an example

¹Laboratoire de Météorologie Physique, Clermont Université, Université Blaise Pascal, Clermont-Ferrand, France.

²CNRS, INSU, UMR 6016, Aubière, France.

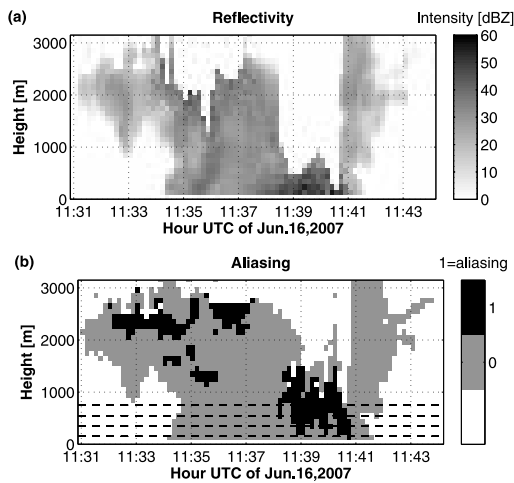


Figure 1. Time-height plot of (a) reflectivity and (b) aliasing detection. The horizontal dashed lines in Figure 1b show the height of the measurements presented in Figure 2.

to support our study. During this rain event, a collocated rain gauge measured a rainfall accumulation of 1.5 mm over the 15 min period, with a maximum rain rate of 34 mm h⁻¹ over 1 min. Figure 1a shows the time-height plot of the MRR reflectivity. It exhibits two periods with a marked absence of data above high reflectivity peaks: around 11:35 UTC above 2000 m and around 11:40 UTC above 500 m. These lacks result from data being rejected due to excessive attenuation correction. Indeed, Figure 1b, which will be presented further, show that some signal still allows the aliasing detection in such zones until the total fading of the signal due to attenuation. However, we will show in the following that it is the impact of strong vertical winds that provokes an overestimation of attenuation and, thus, the rejection of otherwise valid data. Hence, to study this effect, we will consider the data derived without attenuation correction.

3.1. Aliasing Description

[10] Figure 2 shows the time evolution of the spectral reflectivity as a function of the Doppler velocity, from 100 m up to 700 m (AGL). On Figure 2a (100 m AGL), ground echoes picked up by sidelobes are visible at the 0 m s⁻¹ speed (bottom) but also aliased beyond 12 m s⁻¹ (top). Being outside the limits of the analyzed range of velocities, these echoes have no impact on the retrieved parameters. We also notice that the spectral reflectivity is getting more intense with increased spectral width in time, in agreement with the precipitation intensification seen in the low level reflectivity evolution of Figure 1a. Besides, three spectra (highlighted by the vertical dashed lines) are very different from the others as a high noise level led to the suppression of part of the signal. Disregarding these three noisy spectra, the lower limit of all spectra is fairly stable. Its variations are small and hence can be due to either variations of the DSD or of the vertical wind.

[11] Looking at the next height (300 m AGL, Figure 2b), the spectra exhibit a noticeably different evolution in time than at 100 m AGL. The most striking is that, around 11:40 UTC, the upper part of the velocity spectra becomes greater than 12 m s⁻¹ and aliases on the low velocity part, indicating fall speed reaching about 13 m s⁻¹. Such fall speeds are impossible except for hail, but in such a case they would still be observed at lower ranges. Furthermore, the lower limit of the spectra also increases, indicating that the entire velocity spectra have been shifted towards higher values, as would be expected with a superimposed downdraft. In addition, such a strong variation is too sudden to be solely explained by DSD variability.

[12] Similar comments can be made for higher heights (Figures 2c and 2d), where the aliasing is even more marked, with vertical winds reaching about 6 m s⁻¹.

3.2. Automatic Detection of Aliasing

[13] An automatic detection scheme has been implemented. It flags spectra crossing the measurements spectral limits over

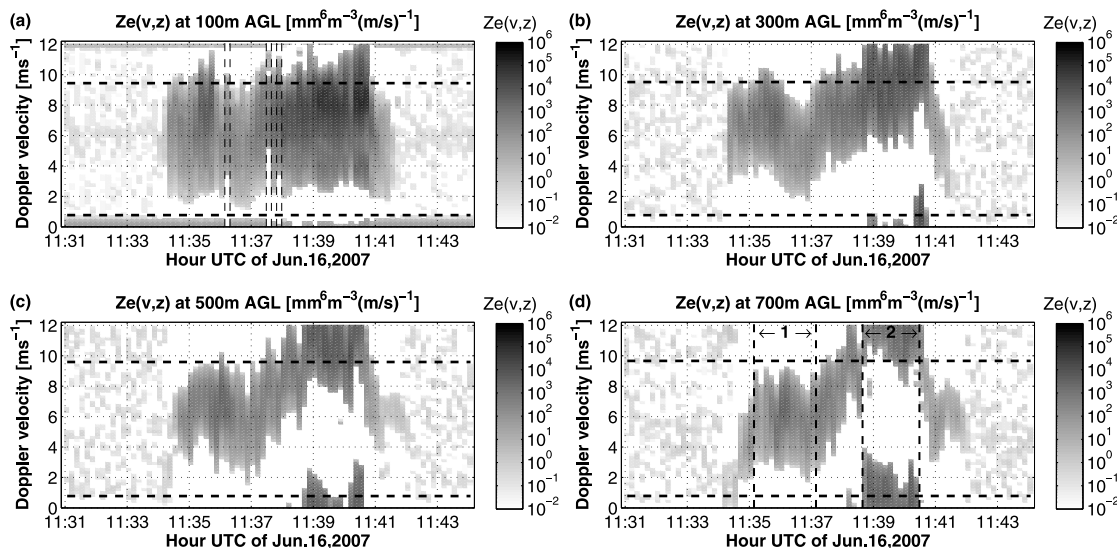


Figure 2. Time evolution of the spectral reflectivity as a function of the Doppler velocity, at (a) 100 m, (b) 300 m, (c) 500 m, and (d) 700 m AGL. The horizontal dashed lines show the limits of the analyzed range.

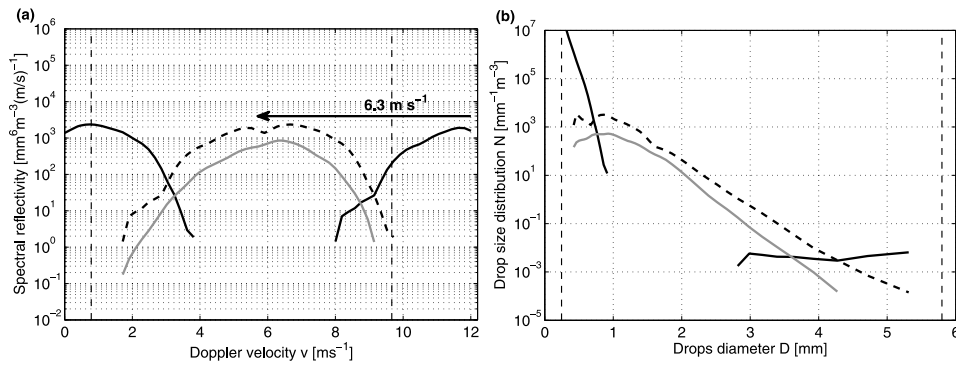


Figure 3. (a) Mean spectral reflectivity as a function of the Doppler velocity at 700 m AGL for the periods delimited in Figure 2d in gray and black for the 1st and 2nd period, respectively. The spectra of the 2nd period, corrected for vertical wind, is plotted in the dashed black line. The thin vertical dashed lines show the limits of the analysed range in Doppler velocity. (b) Same as Figure 3a but for DSDs.

at least 8 Doppler bins. This last test avoids false detection caused by the ground echoes in the lower gates. The result of this detection scheme applied to the time-height plot of Figure 1a is shown in Figure 1b. We recognize the occurrence of aliased spectra at the heights corresponding to the plots of Figure 2. Additionally, comparing with Figure 1a, aliasing also appears to be linked with data loss associated with strong attenuation. However, a closer look shows that aliasing always appears before (i.e., at lower height), while inspection of some weaker rain cases in our data set reveals aliasing without data suppression due to strong attenuation. Hence, aliasing detection can be used to our benefit to help identify incorrect MRR measurements which would have otherwise been accepted.

[14] Furthermore, such detection could also be used to identify strong vertical winds and issue a warning. For example, assuming a standard DSD with diameters ranging from about 0.5 mm to 4 mm, the corresponding reflectivity spectrum would be limited between about 2 and 9 m s⁻¹ at sea level. Hence, given that the limits of the fall velocity measured by the MRR are 0 and 12 m s⁻¹, aliasing of such a spectrum would be produced by either a downdraft larger than 3 m s⁻¹, or an updraft larger than 2 m s⁻¹.

4. Effect of Aliasing on MRR Retrievals

[15] In order to study the impact of aliasing, we choose two periods of about 2 min with stable spectral reflectivity at 700 m AGL within the case presented in section 3. The 1st period spread from 11:35:14 to 11:37:04 UTC and the 2nd period from 11:38:44 to 11:40:24 UTC (vertical dashed lines in Figure 2d).

4.1. On Spectral Reflectivity

[16] As discussed in section 3, the variation with height of the spectrum is somewhat low during the 1st period, and hence, we can assume that, wind and DSD vertical variabilities are negligible. On the other hand, the supposedly strong downdraft of the 2nd period shifts the spectrum towards larger velocities leading to aliasing. The mean spectra of the two periods are plotted in Figure 3a. It is worth noting that because of the vertical wind, the maximum value in the aliased spectrum is near the lower limit of the analysed range. Also plotted in Figure 3 is this last spectrum corrected for an estimated downdraft of 6.3 m s⁻¹ such that its spectral reflectivity best matches the one at

100 m AGL (Figure 2a). In this estimation, the error due to neglecting the DSD vertical variability is at most of the order of 1 m s⁻¹. It can be shown that this error will not affect the overall results in comparison with the error due to aliasing. The corrected spectrum has a slightly larger width and higher reflectivities at all velocities compared to the 1st period spectrum. This is in agreement with the precipitation intensification in time. On the other hand, the very similar shape of these two spectra is striking, further confirming the validity of the correction.

4.2. On DSD

[17] Given the height of the melting layer (2000 m AGL) somewhat visible as a bright band around 11:42 on Figure 1a as the rain become stratiform, the only ice phase hydrometeors that can be present at 700 m AGL would be wet hail, even within downdraft of the 2nd period. However, the measured reflectivity for wet hail would be considerably higher (above 55 dBZ) than the one observed in Figure 1a and from the data of a nearby scanning X-band radar (see Movie S1 of the auxiliary material).¹ Therefore, we can assume that only liquid phase remains.

[18] The three mean reflectivity spectra of section 4.1 are used to derive the corresponding DSDs (Figure 3b). Due to aliasing, the shape of the 2nd period DSD is unrealistic for numerous reasons: firstly, it is in two separate parts, secondly, in order to reach the high reflectivity of the spectrum near the lower limit of the analyzed range, the left part has a very high concentration of small drops (more than 10⁵ mm⁻¹ m⁻³), thirdly, the right part has a nearly flat slope as opposed to the usual exponential decrease. By contrast, the DSD derived from the corrected spectrum, is very similar to the 1st period one with slightly higher concentrations of all drop sizes.

[19] To further validate the corrected DSD, we derived its gamma parameterization by using the methods of moments [Tokay and Short, 1996]. We used high moments of DSD (4th, 5th and 6th) on the basis that they are the most accurate, as the DSD retrieval is based on reflectivity measurements. This leads to the parameters $N_0 = 1.19 \times 10^6$, $\lambda = 6.4$ and $\mu = 3.8$ and to the corresponding relationship $Z = 802R^{1.28}$. All these values are effectively in the range found

¹Auxiliary materials are available in the HTML. doi:10.1029/2010GL046018.

Table 1. Radar Reflectivity Factor Z , Rainrate R , and Attenuation Coefficient k Calculated From the Aliased and Corrected DSDs of Figure 3b

	Z (mm ⁶ m ⁻³)	R (mm h ⁻¹)	k (dB km ⁻¹)
“Aliased DSD”	34.7	205.9	22.5
Corrected DSD	37.2	18.8	1.7

in literature, while the large prefactor and small exponent are consistent with a convective Z - R relationship. Finally, we can assume from Figure 3 that averaging DSDs over long time period without checking the presence of aliasing would lead to an incorrect concave upward DSD.

4.3. On the Retrieved Parameters

[20] As the aliased spectrum retrieved DSD has an excess of small and large drops and a deficit of medium drops, the impact on the retrieved parameters of interest (Z , R and k) is non-trivial. Therefore, we computed the different parameters from the “aliased” and corrected DSDs of section 4.2. Table 1 lists the resulting values. First, since the spectral reflectivity has only been shifted, Z derived from the two spectra should not differ. However, as a part of the aliased spectrum fall outside the analyzed range, the reflectivity of “aliased DSD” is lower by about 2.5 dBZ. Second, because of their very high concentration, drops with D lower than 0.5 mm in the “aliased DSD” dominate the contribution on R which is then strongly overestimated. Hence, such data would be considered outliers if we used these MRR measurements to derive Z - R relationships as was done by *Van Baelen et al.* [2009]. Finally, k is also strongly overestimated preventing from further correction as it exceeds the maximum value allowed. Thus, in this example, as in most of the cases of data loss associated with excessive attenuation correction, aliasing is the cause. Hence, extending our aliasing detection scheme with one for vertical wind mitigation would allow for correct continuous measurements in these cases.

5. Frequency of Occurrence of Aliasing

[21] In order to get a better feeling for the overall influence of aliasing on day to day operation of the MRR, we have considered all the rain periods of the corresponding three month campaign. The vertical wind correction used for the event so far studied cannot be generalized, hence, we investigate the frequency of occurrence of aliasing as a function of the event-average rain gauge rain rate. Three cases have significant mean rain rates (above 4 mm h⁻¹). They correspond to intense showers and hence they show a fairly large relative number of aliased spectra (between 10% and 50%). In the remaining forty cases, six light showers have a significant portion of aliased spectra (between 5% and 20%) but with a weak mean rain rate (about 1 mm h⁻¹). Furthermore, four long and common (about 3 mm h⁻¹) rain events of stratiform precipitation with embedded convection show a low relative number of aliased spectra whereas aliasing would still be a problem in the convective zones. Finally, this statistical study shows that almost a third of the rain events of our data set is concerned by the aliasing problem.

6. Conclusions

[22] In this work, we have shown that strong vertical winds can corrupt the MRR retrievals through reflectivity

spectrum aliasing. As a result, the DSD spectrum retrieved, even when averaged over a few minutes, present abnormal shapes with unrealistic concentrations of small and large drops. As a consequence, the derived parameters Z , R , and k can suffer large errors. In particular, k can be largely over-estimated and lead to data rejection as rain attenuation correction appears no longer valid. Such anomalies can take place during marked convective rain cases but also under less intense rain conditions.

[23] Hence, reflectivity spectrum aliasing can be identified automatically even when there is no apparent effect on the attenuation. Thus, this detection can be used to eliminate incorrect MRR retrievals associated to large vertical winds. Indeed, we have shown that, under the assumption of a standard DSD, we could identify vertical winds of the order and above about 2 m s⁻¹ for updrafts and 3 m s⁻¹ for downdrafts.

[24] Unfortunately, as shown by *Atlas et al.* [1973], errors in the vertical wind of 1 m s⁻¹ can already be crippling for the DSD estimation. Hence, the detection of aliasing anomalies can be used to eliminate data from strong convective cases. However, in the presence of moderate vertical winds in the range of 1 to 2 m s⁻¹, an adapted detection procedure is still needed if one wants to use the instantaneous MRR retrievals rather than one minute averaged values.

[25] **Acknowledgments.** We thank two anonymous reviewers for their very helpful comments in improving the manuscript. The first author acknowledges financial support from the CNRS and the “Conseil Régional d’Auvergne.”

References

- Atlas, D., R. C. Srivastava, and R. S. Sekhon (1973), Doppler radar characteristics of precipitation at vertical incidence, *Rev. Geophys.*, *11*, 1–35.
- Babb, D. M., J. Verlinde, and B. W. Rust (2000), The removal of turbulent broadening in radar Doppler spectra using linear inversion with double-sided constraints, *J. Atmos. Ocean. Technol.*, *17*, 1583–1595.
- Battan, L. J. (1964), Some observations of vertical velocities and precipitation sizes in a thunderstorm, *J. Appl. Meteorol.*, *3*, 415–420.
- Gossard, E. E. (1994), Measurement of cloud droplet size spectra by Doppler radar, *J. Atmos. Ocean. Technol.*, *11*, 712–726.
- Hauser, D., and P. Amayenc (1981), A new method for deducing hydrometeor-size distributions and vertical air motions from Doppler radar measurements at vertical incidence, *J. Appl. Meteorol.*, *20*, 547–555.
- Hitschfeld, W., and J. Bordan (1954), Errors inherent in the radar measurements of rainfall at attenuating wavelengths, *J. Atmos. Sci.*, *11*, 58–67.
- Peters, G., B. Fischer, H. Münster, M. Clemens, and A. Wagner (2005), Profiles of raindrop size distributions as retrieved by Microrain Radars, *J. Appl. Meteorol.*, *44*, 1930–1949.
- Peters, G., B. Fischer, and M. Clemens (2010), Rain attenuation of radar echoes considering finite-range resolution and using drop size distributions, *J. Atmos. Ocean. Technol.*, *27*, 829–842.
- Rogers, R. R. (1967), Doppler radar investigations of Hawaiian rain, *Tellus*, *19*, 432–455.
- Tokay, A., and D. A. Short (1996), Evidence from tropical raindrop spectra of the origin of rain from stratiform versus convective clouds, *J. Appl. Meteorol.*, *35*, 355–371.
- Van Baelen, J., F. Tridon, and Y. Pointin (2009), Simultaneous X-band and K-band study of precipitation to derive specific Z - R relationships, *Atmos. Res.*, *94*, 596–605.
- Wakasugi, K., A. Mizutani, M. Matsuo, S. Fukao, and S. Kato (1987), Further discussion on deriving drop-size distribution and vertical air velocities directly from VHF Doppler radar spectra, *J. Atmos. Ocean. Technol.*, *4*, 170–179.

Y. Pointin, F. Tridon, and J. Van Baelen, Laboratoire de Météorologie Physique, Clermont Université, 24 avenue des Landais, F-63177 Aubière, France. (F.Tridon@opgc.univ-bpclermont.fr)